Am J Transl Res 2017;9(9):3904-3917
www.ajtr.org /ISSN:1943-8141/AJTR0062793

Original Article

Comprehensive analysis of long non-coding RNA PVT1 gene interaction regulatory network in hepatocellular carcinoma using gene microarray and bioinformatics

Yu Zhang[1*], Yi-Wu Dang[1*], Xiao Wang[2], Xia Yang[1], Rui Zhang[1], Zi-Li Lv[1*], Gang Chen[1*]

[1]Department of Pathology, First Affiliated Hospital of Guangxi Medical University, 6 Shuangyong Road, Nanning 530021, Guangxi Zhuang Autonomous Region, China; [2]Department of Orthopedics, Shandong Provincial Hospital affiliated to Shandong University, Jinan 250012, Shandong Province, China. [*]Equal contributors.

Received April 15, 2017; Accepted August 17, 2017; Epub September 15, 2017; Published September 30, 2017

Abstract: PVT1 has been reported to be involved in the tumorigenesis and development of different cancers. However, the role of PVT1 in hepatocellular carcinoma (HCC) remains unclear. In this study, we applied gene microarray analysis to detect differentially expressed genes (DEGs) between PVT1 RNAi groups and controls. We initially investigated and confirmed PVT1 expression in HCC using The Cancer Genome Atlas (TCGA). The potential genes and pathways associated with PVT1 were also analyzed. We also performed bioinformatics analyses (Gene Ontology (GO), pathway, Kyoto Encyclopedia of Genes and Genomes (KEGG), and network analyses) to explore the underlying pathways and networks of these potential genes. We selected DLC1 for further analysis. Based on the TCGA database, PVT1 was markedly up-regulated in HCC, whereas DLC1 was down-regulated. Moreover, PVT1 expression negatively correlated with DLC1 in HCC, an observation that has been further validated in different cohorts with Oncomine. High expression of PVT1 was positively associated with gender, race, vascular invasion and pathological grade in HCC. Additionally, the ROC curve indicated that both PVT1 and DLC1 have high diagnostic value in HCC. We speculated that PVT1 might play a significant role in HCC development and progression via regulation of various pathways and genes, especially DLC1 and the Hippo signaling pathway. However, this mechanism should be confirmed by functional experiments.

Keywords: PVT1, HCC, gene microarray, TCGA, GO, KEGG

Introduction

Hepatocellular carcinoma (HCC) remains the most common liver malignancy worldwide, with an extremely high mortality rate [1-4]. In China, chronic infection of hepatitis B virus (HBV) has become the leading cause of HCC [2, 5]. Though the most effective treatment is surgery, including liver transplantation and tumor resection, high rates of metastasis and postoperative recurrence remain an obstacle for long-term survival of HCC patients [6-9]. As current treatment strategies are unsatisfactory, it is essential to explore the underlying mechanism of HCC, which might provide novel insights for the diagnosis and treatment of HCC patients.

Long non-coding RNAs (lncRNAs) refer to non-protein coding RNAs with a length varying from 200 nucleotides to 100 kilobases [10-12]. Various lncRNAs have been demonstrated to play significant roles in epigenetic gene regulation, transcriptional regulation, and disease development [13-15]. More importantly, due to their wide distribution in the nucleus, lncRNAs can regulate the transcription of adjacent genes by combining the transcription factors or polymerases [16-18]. Accumulating evidence has confirmed that differential lncRNA expression could affect the progression of HCC by regulating the self-renewal ability of liver cancer stem cells and other biological functions, including proliferation, invasion, metastasis and apoptosis [19-22]. Moreover, several publications have reported that the ectopic expression of lncRNAs might be related to chemotherapy resistance seen in HCC patients [23, 24].

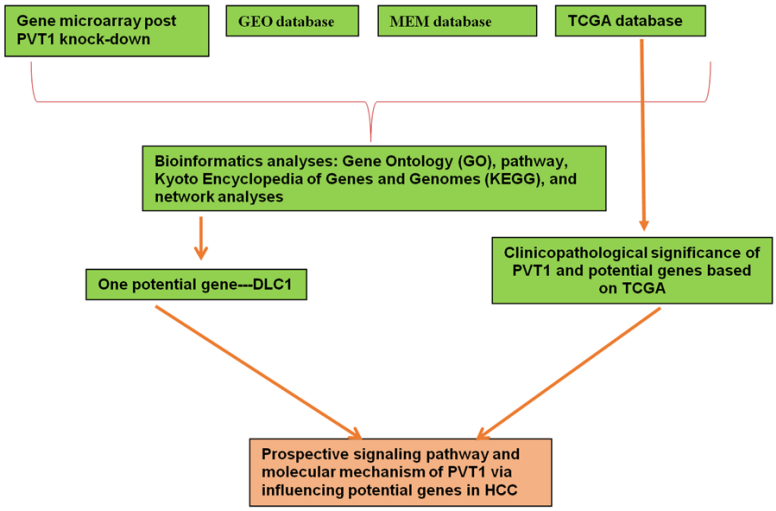

Figure 1. Flow chart of this study. To explore the different expression of PVT1 in HCC and normal liver, we combined the gene expression profile with silencing PVT1 expression and GEO, TCGA and MEM databases to explore the potential genes related to PVT1. Bioinformatics analyses, including GO, KEGG and network analysis, were applied to investigate the potential functions, pathways and networks of the potential genes. The clinicopathological significance of PVT1 and the potential genes was also explored based on TCGA.

LncRNA PVT1 is located on 8q24, a known cancer-related region [25]. PVT1 functions as an oncogene by participating in DNA rearrangement or through interacting with MYC and encoding microRNA [26]. Several studies have confirmed that overexpression of PVT1 could accelerate the development and progression of cancers and reduce the chemosensitivity of cancer patients [27-31]. Although it has been shown that PVT1 exhibits high expression in HCC, promotes proliferation and predicts recurrence compared with normal tissues, the functions and mechanism of tumor formation and progression with respect to PVT1 in HCC remain elusive [32-34].

In the present study, we sought to explore the differential expression of PVT1 in HCC and normal liver. Furthermore, we combined the gene expression profile with a silenced PVT1 expression profile and used Gene Expression Omnibus (GEO), The Cancer Genome Atlas (TCGA), and Multi Experiment Matrix (MEM) databases to explore potential genes related to PVT1 in HCC. Bioinformatics analysis, including Gene Ontology (GO), Kyoto Encyclopedia of Genes and Genomes (KEGG) and network analysis, were applied to investigate the potential functions, pathways and networks of identified genes of interest [35-38]. A flow chart of this study is shown in **Figure 1**.

Material and methods

Cell culture and siRNA transfection

The human HCC cell line SMMC-7721 was purchased from American Type Culture Collection (ATCC), and all cells were cultured in Dulbecco's Modified Eagle's Medium (DMEM) supplemented with 10% fetal bovine serum (FBS) and 1% penicillin/streptomycin at 37°C with 5% CO_2 in a humidified incubator. The Lenti-siRNA vector for PVT1 was synthesized by GeneChem (Shanghai, China) (sense: 5'-CCCAACAGGAGGACAGCUUTT-3'; antisense: 5'-AAGCUGUCCUCCUGUUGGGTT-3'). SiRNA vectors of PVT1 were transfected into HCC cell lines based on the manufacturer's protocol.

Gene microarray analysis

The gene microarray hybridization and sample analysis were performed by Kangchen Bio-tech (Shanghai, China). Briefly, mRNA was extracted from the total RNA after removing the rRNA (mRNA-ONLY Eukaryotic mRNA Isolation Kit, Epicentre Biotechnologies, Madison, USA). Then, a random priming method was used to transcribe and amplify the RNA into fluorescent cRNA. The Human MRNA Array v3.0 (8 × 60 K, Arraystar, Rockville, MD, USA) was utilized to label and cross cRNAs. The Agilent Feature Extraction software (version 11.0.1.1) was used to obtain the original data. Quantile normalization and data analysis were conducted by the GeneSpring GX v12.1 (Agilent Technologies). Differentially expressed genes (DEGs) between PVT1 RNAi and control groups were identified as a fold change (FC)≥2, and P≤0.05 was the cut-off.

Identification of potential genes and pathways associated with PVT1

To further analyze the potential genes, pathways and functions associated with PVT1, three

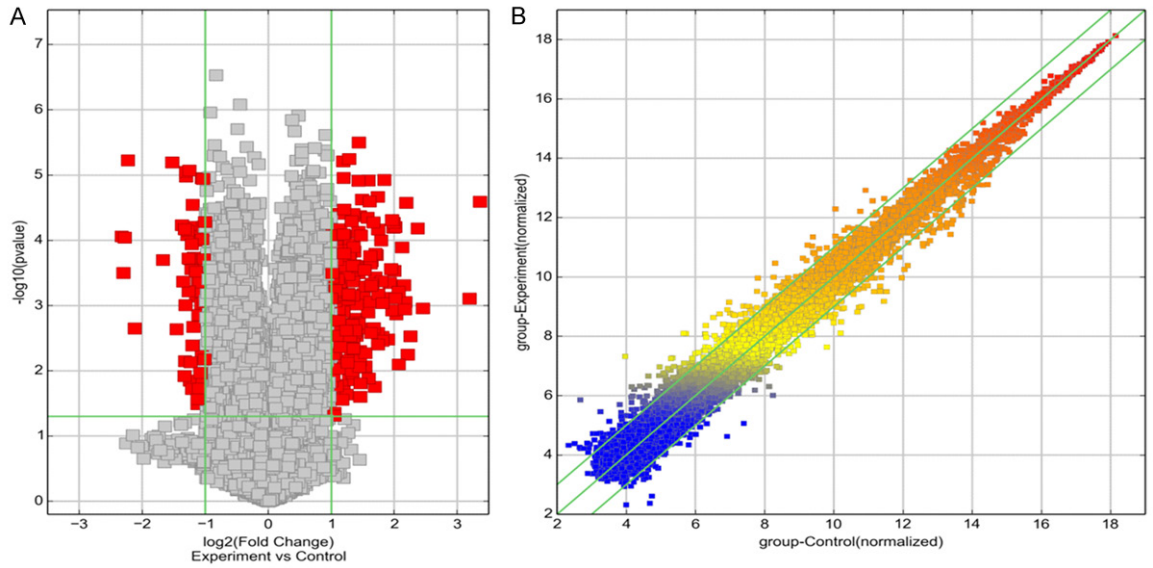

Figure 2. Gene clip after PVT1 knock-down in HCC. A. Volcano plot of differentially expressed genes in PVT1-control and PVT1-RNAi groups; red dots indicate differentially expressed genes with |FC|≥2 and P≤0.05. Gray dots indicate genes with expression of |FC|<2 or P>0.05. One hundred ninety-five up-regulated genes and 60 down-regulated genes were significantly differentially expressed in the PVT1-control and PVT1-RNAi groups with fold change ≥2, P≤0.05. B. Box-scatter plot of differentially expressed genes in PVT1-control and PVT1-RNAi groups; the X axis represents the normalized mean value of the PVT1-control group, and the Y axis represents the normalized mean value of the PVT1-RNAi group.

databases were used to further explore differentially expressed or co-expressed genes. We selected the genes differentially expressed in GEO (http://www.ncbi.nlm.nih.gov/geo/) database, The TCGA database, the genes associated with PVT1 in TCGA database, the co-expressed genes of PVT1 in MEM (http://biit.cs.ut.ee/mem/index.cgi) and the DEGs after the knock-down of PVT1 [39-42]. Candidate genes were identified based on Venn diagrams (http://bioinformatics.psb.ugent.be/webtools/Venn/). In addition, bioinformatic analyses, including GO, KEGG and network analysis, were applied to investigate the underlying functions, pathways and networks of these genes as described [1, 43, 44]. The DAVID Bioinformatics Tool (https://david.ncifcrf.gov/, version 6.7) 50 and KOBAS 2.0 (http://kobas.cbi.pku.edu.cn/) were used for GO and KEGG analyses. Three categories were exported from GO analysis: biological process (BP), cellular component (CC) and molecular function (MF). In addition, Cytoscape (version 2.8, http://cytoscape.org) was applied to determine the functional network between PVT1 and these potential genes.

Validation of the expression of PVT1 and potential genes

Clinical data of HCC patients were obtained from TCGA database. The relationship between PVT1 and potential gene expression and the clinical pathological parameters in HCC was identified based on the original data in TCGA database. Furthermore, the Oncomine (https://www.oncomine.org/) database was also used to verify the expression of PVT1 and DLC1 [45].

Statistical analysis

SPSS 22.0 was used for statistical analysis. The mean ± standard deviation (Mean ± SD) was used to estimate expression. PVT1 expression in HCC versus normal liver was evaluated by Student's t-test. Student's t-test was also utilized to evaluate the difference between PVT1 expression and the clinicopathological parameters. Comparisons between subgroups were performed using one-way analysis of variance (ANOVA). The Spearman test was used to investigate the correlation between PVT1 and the potential genes. In addition, the ROC curve was employed to predict clinical diagnostic

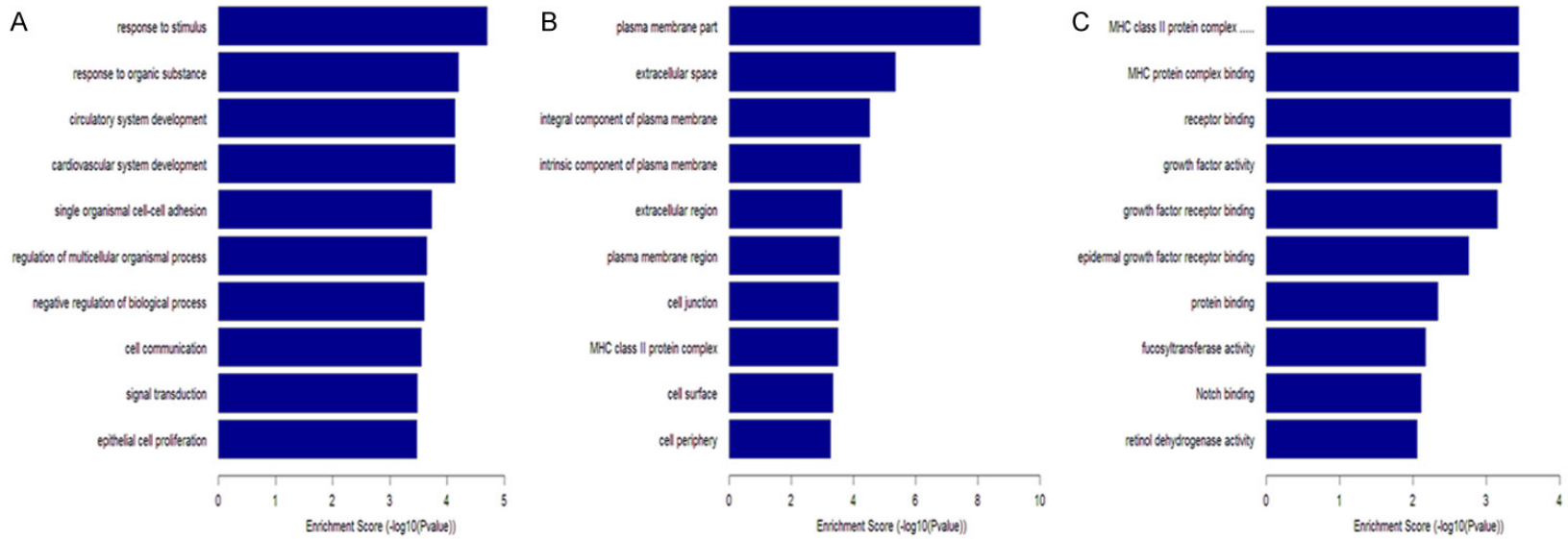

Figure 3. Distribution of GO terms for up-regulated genes in HCC. These results show the most strongly enriched GO terms of the up-regulated genes. A. Biological process (BP). B. Cellular component (CC). C. Molecular function (MF).

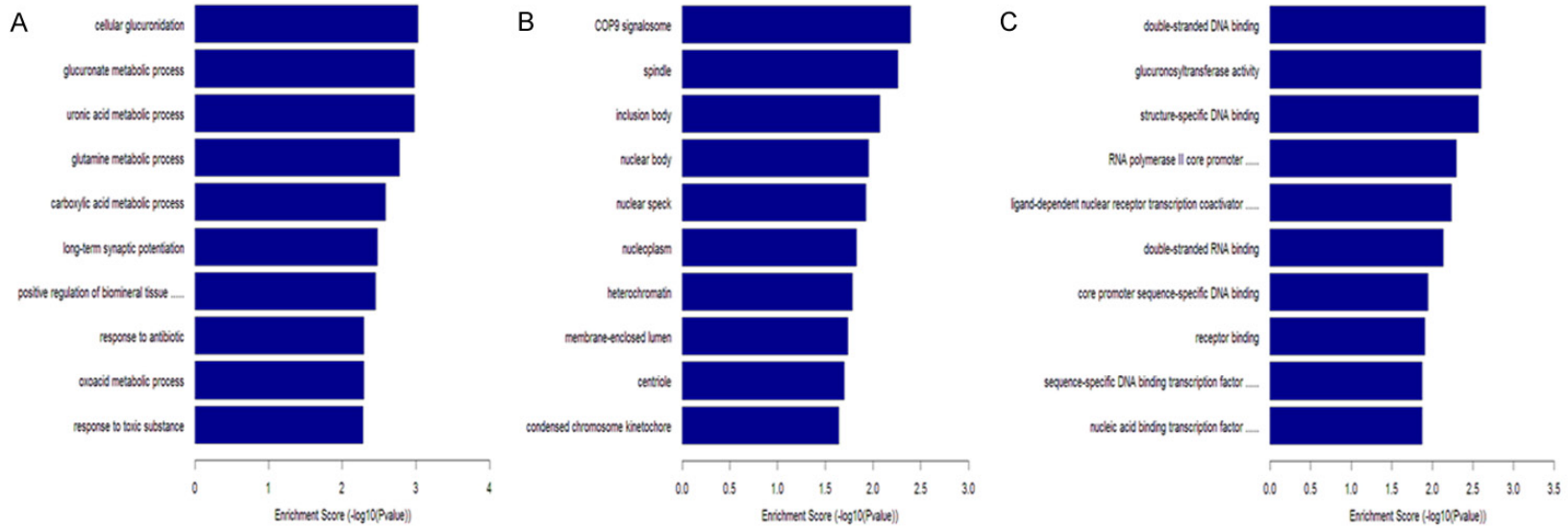

Figure 4. Distribution of GO terms for down-regulated genes in HCC. These results show the most strongly enriched GO terms of the down-regulated genes. A. Biological process (BP). B. Cellular component (CC). C. Molecular function (MF).

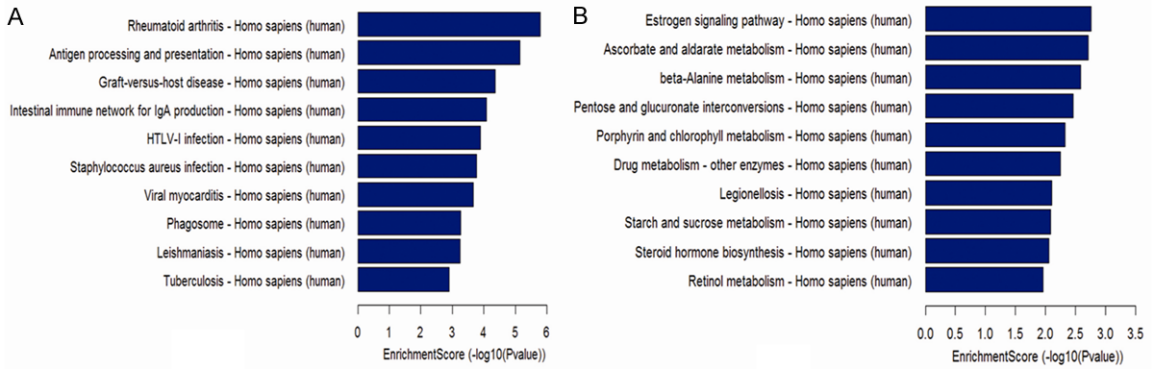

Figure 5. Distribution of KEGG terms for the differentially expressed genes in HCC. These results showed the most strongly enriched KEGG terms of the differentially expressed genes in HCC. A. Up-regulated genes. B. Down-regulated genes.

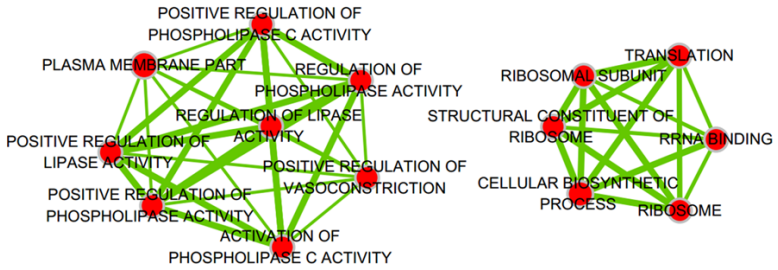

Figure 6. A function network of Gene Ontology (GO) terms for the potential genes of PVT1 in HCC. A function network was constructed according to Cytoscape.

value of PVT1 and the potential genes in HCC. $P<0.05$ (two-sides) was considered statistically significant.

Results

Potential genes regulated by the PVT1

A gene microarray analysis was used to detect differential expression profiles between PVT1 and PVT1 RNAi in three paired groups of SMMC-7721 cells. One hundred ninety-five up-regulated genes and 60 down-regulated genes were significantly differentially expressed in the PVT1-control and PVT1-RNAi groups with $|FC|\geq 2$, $P\leq 0.05$ (**Figure 2**). All up-regulated and down-regulated genes were analyzed with GO and KEGG. Results showed that the up-regulated genes were strongly enriched in response to the stimulus, plasma membrane part binding and MHC protein complex binding, whereas the down-regulated genes were strongly enriched in cellular glucuronidation, COP9 signalosome, and double-stranded DNA binding (**Figures 3**, **4**). In addition, the KEGG analysis clarified the most significant pathways, including the estrogen signaling pathway, ascorbate and aldarate metabolism, antigen processing and presentation, and so on (**Figure 5**).

Based on the MEM database, the top 2,000 co-expressed genes of PVT1 in three different probe sets (216240_AT, 1558290_A_AT and 1562153_A_AT) were selected for further analysis. Among these co-expressed genes, 3626 genes were predicted by at least one probe set. To identify key genes in HCC, we downloaded one gene expression profile (GSE57786) from the GEO database. A total of 12,018 DEGs were screened out. Additionally, the TCGA database was utilized to select the genes associated with PVT1 and the DEGs in HCC. As a result, 60,244 genes were identified as DEGs, and 1,313 genes associated with PVT1 were screened out. Interestingly, only one

Table 1. Top 5 enrichment GO terms (BP, CC, and MF) from the microarray data

GO:ID	Term	Ontology	Enrichment score	P	Gene symbol
GO:0006412	Translation	BP	5.40966	0.001796	RSL1D1, MRPL52, SLC25A32, RPS18, RPL30, RPL5, RPL22L1
GO:0045907	Positive regulation of vasoconstriction	BP	24.92308	0.006163	AVPR1A, ADRA1A, DBH
GO:0034605	Cellular response to heat	BP	17.33779	0.012561	HSF1, HTRA2, ANO1
GO:0098609	Cell-cell adhesion	BP	7.935706	0.013634	EPCAM, RSL1D1, YWHAZ, OLA1
GO:0050714	Positive regulation of Protein secretion	BP	16.61538	0.013637	KCNN4, PPIA, ANG
GO:0016020	Membrane	CC	2.934011	6.35E-05	DLC1, ABCE1, DARS, AIMP1, OLA1, ITGB2, RSL1D1, DDX56, RPL30, RPS18, FAM49B, PPIA, RPL8, FARSB, RBM19, PABPC1, KSR1, TMPRSS13, APBA1
GO:0022625	Cytosolic large ribosomal subunit	CC	13.26555	8.42E-05	RSL1D1, RPL30, RPL8, RPL5, RPL22L1, MRTO4
GO:0005925	Focal adhesion	CC	3.504108	0.007635	DLC1, YWHAZ, RPS18, RPL30, NME2, PPIA, RPL8, PABPC1
GO:0070062	Extracellular exosome	CC	1.675067	0.008663	YWHAZ, GNPDA1, ANO1, ITGB2, SYT7, APLP2, SCRIB, CMBL, EPCAM, ATP2B2, RPL30, FAM49B, CLCF1, PABPC1, SLC39A4, GNG7, TECTA, DARS, SLC22A8, OLA1, RPS18, CCT4, PPIA, ZNHIT6, GDF15, FABP5
GO:0005730	Nucleolus	CC	2.532514	0.010996	RSL1D1, DDX56, MTDH, NCF2, ANG, RPL8, PAK1IP1, RBM19, OLA1, RPL5, MRTO4
GO:0003735	Structural constituent of ribosome	MF	5.504157	2.15E-04	MRPL52, SLC25A32, RPS18, RPL30, RPL8, RPL5, MRPS21, RPL22L1, MRTO4
GO:0044822	Poly(A) RNA binding	MF	2.31524	0.004573	YWHAZ, MTDH, DARS, ZC3HAV1, UBE2I, MRTO4, RSL1D1, RPL30, DDX56, RPS18, CCT4, PPIA, RPL8, RBM19, PABPC1
GO:0005524	ATP binding	MF	1.906669	0.010918	CIITA, ABCE1, DARS, OLA1, UBE2I, ACACB, DGUOK, MTHFD1L, ABCG8, ATP2B2, DDX56, NME2, ABCC9, CCT4, GSK3B, FARSB, KSR1, RUNX1
GO:0098641	Cadherin binding involved in cell-cell adhesion	MF	7.978675	0.013408	EPCAM, RSL1D1, YWHAZ, OLA1
GO:0005515	Protein binding	MF	3.88184	0.038969	NME2, ANG, TPPP, ITGB2, PABPC1

BP: biological process; CC: cellular component; MF: molecular function.

Table 2. The most important enriched pathway terms from the microarray data

Pathway ID	Definition	Enrichment_Score	P	Gene symbol
bta03010	Ribosome	5.75487	0.00346	RPS18, RPL30, RPL8, RPL5, MRPS21, RPL22L1
bta04970	Salivary secretion	6.193996	0.025342	KCNN4, ATP2B2, ADRA1A, PLCB2
bta04970	Hippo signaling pathway	4.255809	0.027938	YWHAZ, GSK3B, ITGB2, PPP2R2C, SCRIB
bta05134	Legionellosis	6.764496	0.070226	HSF1, ITGB2, NFKB2
bta04728	Dopaminergic synapse	4.016419	0.074198	GSK3B, PLCB2, PPP2R2C, GNG7
bta05200	Pathways in cancer	2.249195	0.083702	GSK3B, LPAR2, TCEB1, NFKB2, RUNX1, PLCB2, GNG7
bta04261	Adrenergic signaling in cardiomyocytes	3.570151	0.097407	ATP2B2, ADRA1A, PLCB2, PPP2R2C

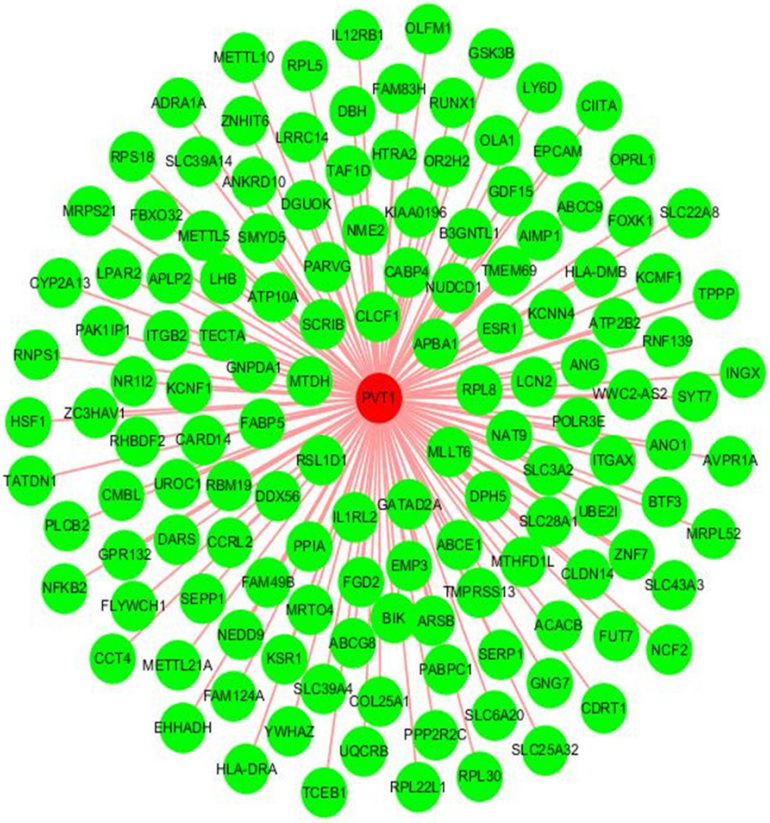

Figure 7. Network analysis between PVT1 and the potential candidate genes. A gene network of the 139 genes was constructed based on Cytoscape. The relationships between PVT1 and the potential genes were easily observed from this network.

gene, DLC1, was selected based on all the aforementioned genes.

GO and pathway analysis

Based on the aforementioned genes, 139 genes were screened and submitted for GO and pathway analyses. The most strongly enriched terms were identified as follows: translation, cell-cell adhesion, nucleolus and poly (A) RNA binding. To further elucidate the functions of these genes, a function network was constructed according to the GO analysis (**Figure 6**). Additionally, the KEGG pathway analysis verified that these genes were significantly involved in the Hippo signaling pathway, ribosomes, dopaminergic synapses, and pathways in cancer. The top five most significant GO terms (BP, CC and MF) and the most important enriched KEGG pathway items are displayed in **Table 1** and **Table 2**. Altogether, the GO and KEGG pathway items indicated that PVT1 might participate in the pathophysiological mechanisms of HCC.

In addition, a gene network of the 139 genes was constructed in the current study (**Figure 7**). The relationships between PVT1 and DEGs were easily observed from this network.

Supplementary information from the cancer genome atlas (TCGA) database

To further elucidate the expression of PVT1 and DLC1 and the relationship between the two, a clinical study was performed based on the original data in TCGA. We found that PVT1 was highly expressed in HCC compared to non-cancerous liver tissues (P<0.0001, **Figure 8A**). We also explored the relationship between PVT1 and the clinicopathological parameters of HCC and discovered that high expression of PVT1 is positively related to gender (P=0.012, **Figure 8B**), race (P=0.006, **Figure 8C**), vascular inva-

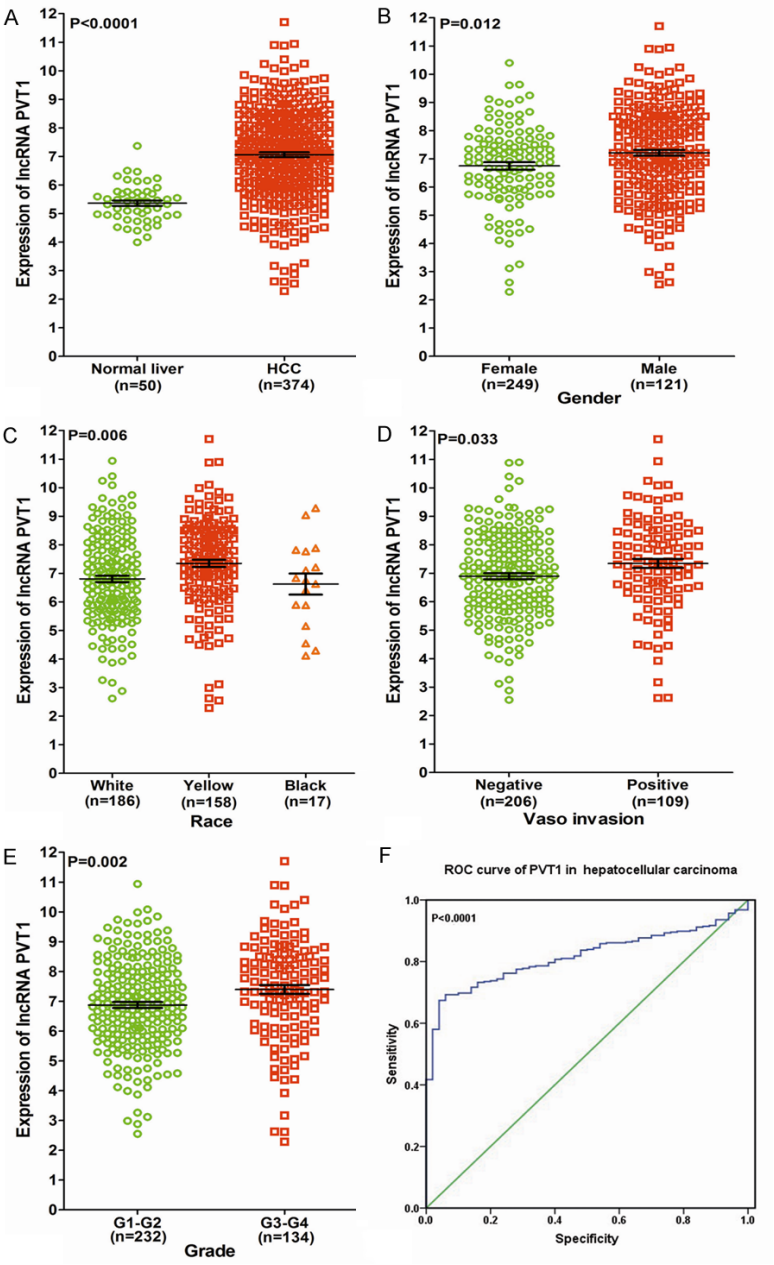

Figure 8. Clinical significance of LncRNA PVT1 in HCC based on TCGA database. A. Differential expression of PVT1 between HCC and non-cancerous liver tissue; B. Differential expression of PVT1 in male vs female; C. White vs Yellow vs Black; D. Non-vascular infiltration vs vascular infiltration; E. G1, G2 vs G3, G4; F. ROC curve of PVT1 in HCC.

sion (P=0.033, **Figure 8D**) and pathological grade (P=0.002, **Figure 8E**, **Table 3**). Additionally, the ROC curve indicates the area under the curve (AUC) of PVT1 was 0.816 (95% CI 0.774~0.859, P<0.0001) for HCC patients, which could place high diagnostic value on PVT1 levels in HCC (**Figure 8F**). We also investigated the relationship between PVT1 expression and other clinical parameters in HCC, but no positive associations were found based on the TCGA database.

Furthermore, DLC1 was down-regulated in HCC based on the TCGA database (P< 0.0001, **Figure 9A**). We also found that the expression of DLC1 was positively related to gender (P=0.011, **Figure 9B**, **Table 4**). Exploring the relationship between DLC1 expression and patient survival, we observed that high DLC1 expression correlated with better survival (51.45± 3.93 months) compared to the low DLC1 expression group (45.42±4.23 months, P=0.253, **Figure 9C**) in HCC. Moreover, the AUC of DLC1 was 0.918 (95% CI 0.883~ 0.954, P<0.0001) for HCC patients, indicating the high diagnostic value of DLC1 levels in HCC (**Figure 9D**). We then compared the expression of PVT1 and DLC1 based on TCGA and found that expression of PVT1 was negatively correlated with DLC1 in HCC (P=-0.063, **Figure 9E**).

Moreover, two cohorts of Chen Liver and Wurmbach Liver from Oncomine were used for validation of PVT1 expression, and the results further confirmed high expression of PVT1 in HCC (**Figure 10**). Likewise, cohorts of Roessler Liver confirmed low expression of DLC1 in HCC, similar to the results obtained from TCGA (**Figure 11**).

Discussion

LncRNAs are involved in regulating biological functions and gene expression in physiological and pathological contexts, such as cancer [16,

Table 3. Differential expression of PVT1 of other clinicopathological parameters in HCC tissue

Clinicopathological features		N	PVT1 expression		
			Mean ± SD	T	*P* value
Tissues	Normal liver	50	5.480±0.704	-11.794	<0.0001
	HCC	374	7.005±1.597		
Age	<60	169	7.058±1.505	0.520	0.603
	≥60	201	6.972±1.668		
Gender	Male	249	7.164±6.722	2.512	0.012
	Female	121	1.644±1.461		
Race	White	186	6.774±1.557	5.239	0.006
	Black	17	6.647±1.590		
	Yellow	158	7.306±1.621		
T(tumor)	T1 + T2	275	7.010±1.528	-0.214	0.831
	T3 + T4	93	7.051±1.804		
Vascular invasion	No	206	6.685±1.532	-2.148	0.033
	Yes	109	7.263±1.618		
Pathological Grade	g1 + g2	232	6.827±.494	-3.079	0.002
	g3 + g4	134	7.358±1.737		
Stage	I + II	257	7.047±1.547	0.198	0.843
	III + IV	90	7.008±1.768		
Recurrence	No	323	7.014±1.622	-1.079	0.281
	Yes	23	7.389±1.378		

46]. Growing evidence has clarified the functions of different lncRNAs in HCC, including lncRNA-PVT1 [19-22, 32]. Overexpression of PVT1 was reported to promote proliferation and invasion of gastric cancer cells through binding to FOXM1, and high PVT1 expression was related to poor prognosis in gastric cancer patients [27]. Liu [28] et al also demonstrated that PVT1 could act as an oncogene in prostate cancer and that PVT1 could activate miR-146a methylation to promote tumor growth. Another study confirmed that PVT1 expression level was positively related to tumor stage and metastasis and that high PVT1 expression could accelerate the progression of epithelial-to-mesenchymal transition in esophageal cancer [47]. In addition, several studies confirmed that the inhibition of PVT1 expression could promote cancer patients' sensitivity to drugs [29, 30, 48]. Nevertheless, the roles of PVT1 in HCC remain elusive.

In our current study, we combine gene microarray analysis with TCGA, GEO and MEM databases to identify potential candidate genes and explore the biological functions of PVT1 in HCC. We found that PVT1 was highly expressed in HCC, which was consistent with the results of Yu et al and Ding et al [32, 33]. This study is the first to show that overexpression of PVT1 is significantly associated with gender, race, vascular invasion and pathological grade in HCC. As a result, our data confirm that PVT1 is up regulated in HCC compared to normal liver tissues based on TCGA database. Additionally, the high AUC of PVT1 predicts diagnostic value in HCC. To date, several studies have reported the expression and functions of PVT1 in HCC. Wang [34] et al found that overexpression of PVT1 promotes proliferation and stem cell-like properties of HCC cells via stabilizing NOP2. Ding [33] et al demonstrated that higher expression of PVT1 was strongly related to AFP level and predicted poor recurrence-free survival. In addition, the result of Yu et al indicated that the combined up-regulation of two lncRNAs (PVT1 and uc002mbe.2) could provide new methodology for diagnosis of HCC, as expression of PVT1 and uc002mbe.2 were positively associated with tumor size and clinical stage in HCC patients [32]. Furthermore, based on the three aforementioned databases, DLC1 was selected for further analysis. We found that DLC1 is down-regulated in HCC based on the TCGA database. We also detected a negative correlation between PVT1 and DLC1 expression in HCC. Many studies have confirmed expression of DLC1 in HCC. For example, song [49] et al verified that DLC1 could be a potential therapeutic target and an independent prognostic marker in HCC. Ng [50] et al demonstrated that DLC1 is a tumor suppressor gene and may play a significant role in hepatocarcinogenesis. In addition, we utilized Oncomine to verify the high expression of PVT1 and the low expression of DLC1 in NCC. GO analysis of the identified candidate genes revealed that they were involved in translation, cell-cell adhesion, nucleolus and poly(A) RNA binding. In addition, the KEGG analysis revealed that

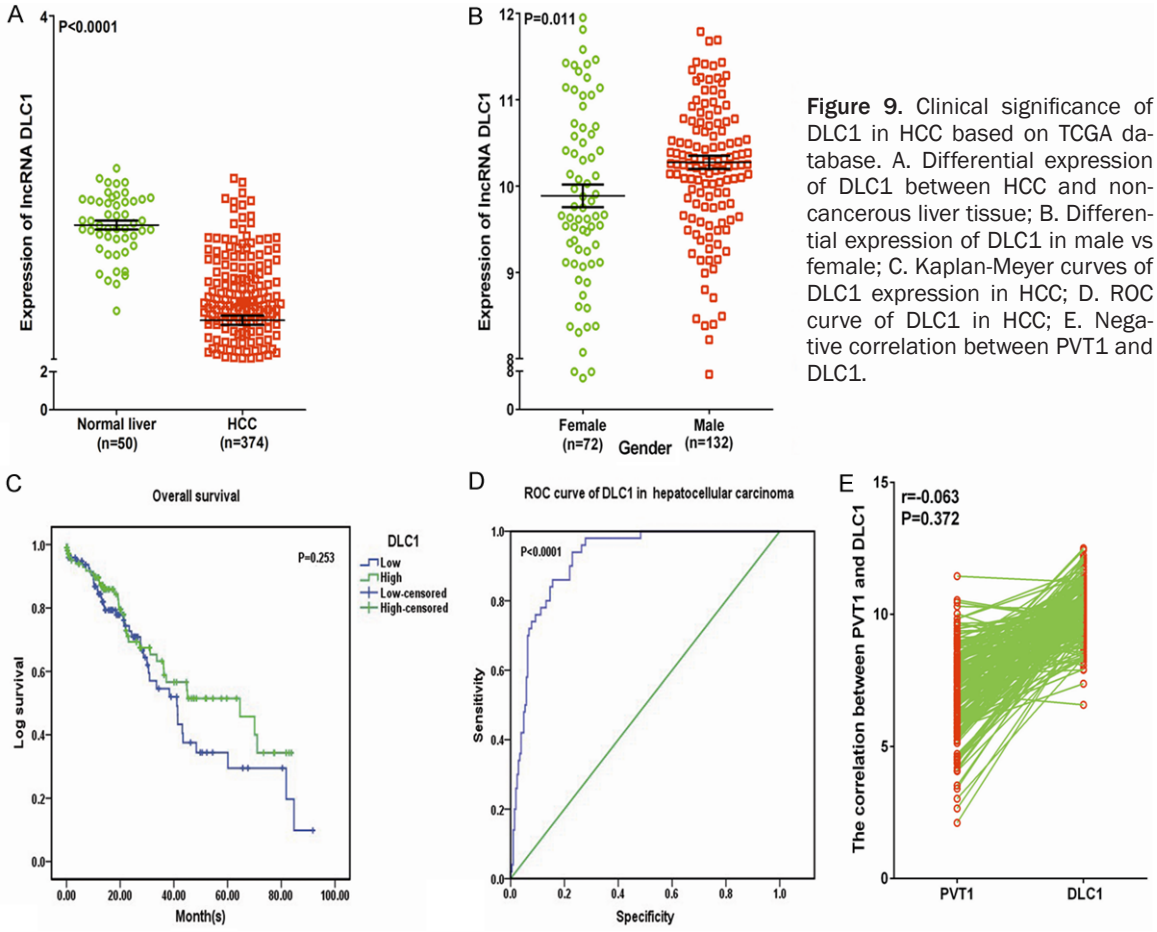

Figure 9. Clinical significance of DLC1 in HCC based on TCGA database. A. Differential expression of DLC1 between HCC and non-cancerous liver tissue; B. Differential expression of DLC1 in male vs female; C. Kaplan-Meyer curves of DLC1 expression in HCC; D. ROC curve of DLC1 in HCC; E. Negative correlation between PVT1 and DLC1.

Table 4. Differential expression of DLC1 in other clinicopathological parameters in HCC tissue

Clinicopathological features		N	DLC1 expression		
			Mean ± SD	T	*P* value
Tissues	Normal liver	50	11.667±0.544	14.873	<0.0001
	HCC	205	10.138±0.977		
Age	<60	83	10.256±1.034	1.415	0.158
	≥60	121	10.059±0.935		
Gender	Male	132	10.276±0.879	2.583	0.011
	Female	72	9.886±1.103		
Race	White	101	10.131±1.022	F=0.297	0.743
	Black	11	10.371±0.684		
	Yellow	87	10.140±0.980		
T (tumor)	T1 + T2	152	10.140±0.974	0.190	0.850
	T3 + T4	50	10.110±1.005		
Vascular invasion	No	108	10.234±0.878	1.263	0.208
	Yes	64	10.052±0.968		
Pathological Grade	g1 + g2	126	10.224±0.956	1.665	0.097
	g3 + g4	74	9.987±0.998		
Stage	I + II	144	10.173±0.992	0.555	0.580
	III + IV	46	10.078±1.048		
Recurrence	No	179	10.129±0.960	0.249	0.804
	Yes	14	10.061±1.298		

these genes were significantly involved in the Hippo signaling pathway, which has been linked to proliferation, tumor formation and prognosis [51-53]. However, further studies are needed to fully identify the mechanism of PVT1 and DLC1 in HCC.

Our findings suggest that PVT1 plays a significant role in HCC. We also show that the PVT1 is associated with gender, race, vascular invasion and pathological grade in HCC. We hypothesized that PVT1 may play a significant role in HCC carcinogenesis and progression by modulating the expression of DLC1 and the Hippo signaling pathway. However, the exact molecu-

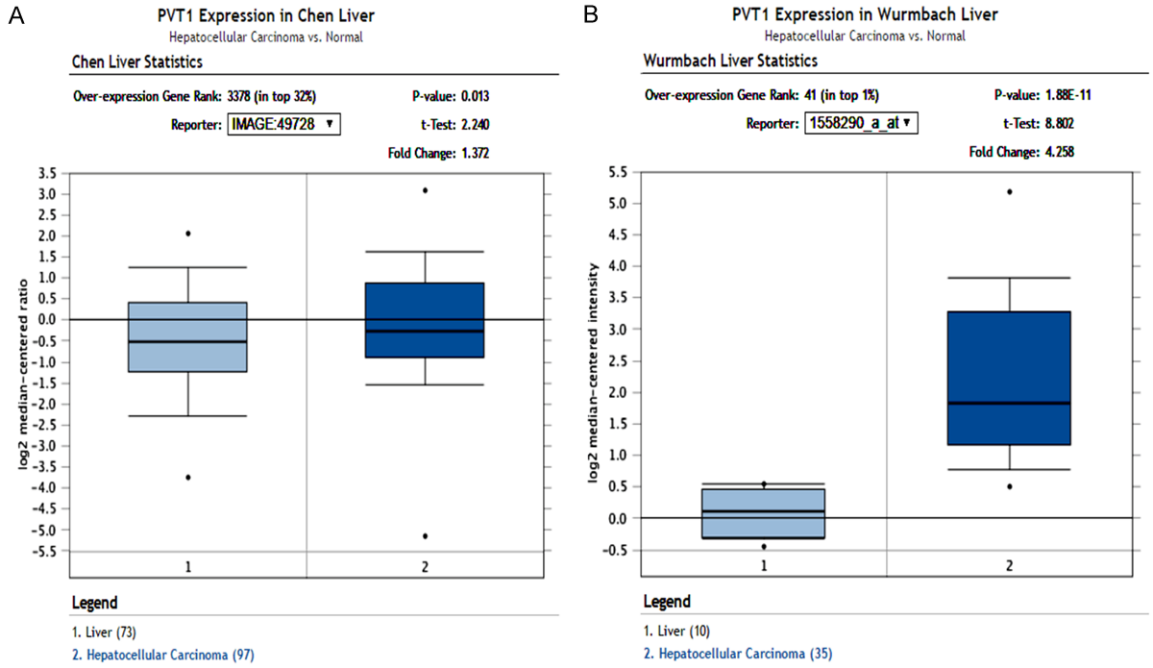

Figure 10. Validation of PVT1 expression in the cohort of Chen Liver and Wurmbach Liver from Oncomine. A. Normal liver tissues (n=73) and hepatocellular carcinoma tissues (n=97) were included in the cohort of Chen Liver; B. Normal liver tissues (n=10) and hepatocellular carcinoma tissues (n=35) were included in the cohort of Wurmbach Liver.

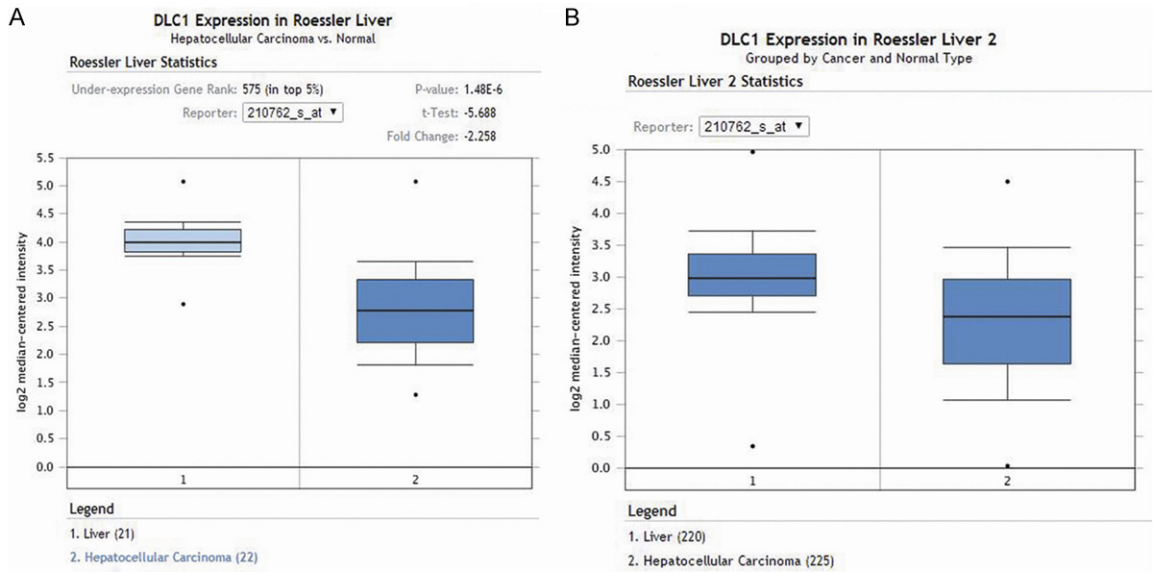

Figure 11. Validation of DLC1 expression in the cohort of Roessler Liver from Oncomine. A. Normal liver tissues (n=21) and hepatocellular carcinoma tissues (n=22) were included in the cohort of Roessler Liver; B. Normal liver tissues (n=220) and hepatocellular carcinoma tissues (n=225) were included in the cohort of Roessler Liver 2.

lar mechanism needs to be verified with future functional experiments.

Acknowledgements

This study was supported by the Fund of National Natural Science Foundation of China (NSFC81560489), the Fund of the Scientific and Technological Research Projects in Guangxi Universities (KY2015YB065) and the Guangxi Medical University Training Program for Distinguished Young Scholars (2017). The authors acknowledge the data provided by the

TCGA database. Yu Zhang and Yi-Wu Dang contributed equally as co-first authors, and Zi-Li Lv and Gang Chen contributed equally as co-corresponding authors of this paper. The funding agencies had no role in the study design, the data collection and analysis, the decision to publish, or the preparation of the manuscript.

Disclosure of conflict of interest

None.

Address correspondence to: Drs. Zi-Li Lv and Gang Chen, Department of Pathology, First Affiliated Hospital of Guangxi Medical University, No. 6 Shuangyong Road, Nanning 530021, Guangxi Zhuang Autonomous Region, China. Email: 15907817634@163.com (ZLL); chen_gang_triones@163.com (GC)

References

[1] Mou T, Zhu D, Wei X, Li T, Zheng D, Pu J, Guo Z and Wu Z. Identification and interaction analysis of key genes and microRNAs in hepatocellular carcinoma by bioinformatics analysis. World J Surg Oncol 2017; 15: 63.

[2] Torre LA, Bray F, Siegel RL, Ferlay J, Lortet-Tieulent J and Jemal A. Global cancer statistics, 2012. CA Cancer J Clin 2015; 65: 87-108.

[3] Li C, Miao R, Liu S, Wan Y, Zhang S, Deng Y, Bi J, Qu K, Zhang J and Liu C. Down-regulation of miR-146b-5p by long noncoding RNA MALAT1 in hepatocellular carcinoma promotes cancer growth and metastasis. Oncotarget 2017; 8: 28683-28695.

[4] Lu PH, Chen MB, Liu YY, Wu MH, Li WT, Wei MX, Liu CY and Qin SK. Identification of sphingosine kinase 1 (SphK1) as a primary target of icaritin in hepatocellular carcinoma cells. Oncotarget 2017; 8: 22800-22810.

[5] Xu Y, Qi Y, Luo J, Yang J, Xie Q, Deng C, Su N, Wei W, Shi D, Xu F, Li X and Xu P. Hepatitis B virus X protein stimulates proliferation, wound closure and inhibits apoptosis of HuH-7 cells via CDC42. Int J Mol Sci 2017; 18.

[6] Moriguchi M, Takayama T, Higaki T, Kimura Y, Yamazaki S, Nakayama H, Ohkubo T and Aramaki O. Early cancer-related death after resection of hepatocellular carcinoma. Surgery 2012; 151: 232-237.

[7] Guo Z, Zhong JH, Jiang JH, Zhang J, Xiang BD and Li LQ. Comparison of survival of patients with BCLC stage a hepatocellular carcinoma after hepatic resection or transarterial chemoembolization: a propensity score-based analysis. Ann Surg Oncol 2014; 21: 3069-3076.

[8] Chiche L, Menahem B, Bazille C, Bouvier V, Plard L, Saguet V, Alves A and Salame E. Recurrence of hepatocellular carcinoma in noncirrhotic liver after hepatectomy. World J Surg 2013; 37: 2410-2418.

[9] Fairman J, Liu KH and Menne S. Prevention of liver tumor formation in woodchucks with established hepatocellular carcinoma by treatment with cationic liposome-DNA complexes. BMC Cancer 2017; 17: 172.

[10] Batista PJ and Chang HY. Long noncoding RNAs: cellular address codes in development and disease. Cell 2013; 152: 1298-1307.

[11] Xie X, Pan J, Wei L, Wu S, Hou H, Li X and Chen W. Gene expression profiling of microRNAs associated with UCA1 in bladder cancer cells. Int J Oncol 2016; 48: 1617-1627.

[12] Sun XJ, Wang Q, Guo B, Liu XY and Wang B. Identification of skin-related lncRNAs as potential biomarkers that involved in Wnt pathways in keloids. Oncotarget 2017; 8: 34236-34244.

[13] Wilusz JE. Long noncoding RNAs: re-writing dogmas of RNA processing and stability. Biochim Biophys Acta 2016; 1859: 128-138.

[14] Yuan X, Wang J, Tang X, Li Y, Xia P and Gao X. Berberine ameliorates nonalcoholic fatty liver disease by a global modulation of hepatic mRNA and lncRNA expression profiles. J Transl Med 2015; 13: 24.

[15] Wei Y and Niu B. Role of MALAT1 as a prognostic factor for survival in various cancers: a systematic review of the literature with meta-analysis. Dis Markers 2015; 2015: 164635.

[16] Ponting CP, Oliver PL and Reik W. Evolution and functions of long noncoding RNAs. Cell 2009; 136: 629-641.

[17] Wang X, Song X, Glass CK and Rosenfeld MG. The long arm of long noncoding RNAs: roles as sensors regulating gene transcriptional programs. Cold Spring Harb Perspect Biol 2011; 3: a003756.

[18] Kugel JF and Goodrich JA. The regulation of mammalian mRNA transcription by lncRNAs: recent discoveries and current concepts. Epigenomics 2013; 5: 95-102.

[19] Zhu P, Wang Y, Wu J, Huang G, Liu B, Ye B, Du Y, Gao G, Tian Y, He L and Fan Z. LncBRM initiates YAP1 signalling activation to drive self-renewal of liver cancer stem cells. Nat Commun 2016; 7: 13608.

[20] Cao C, Sun J, Zhang D, Guo X, Xie L, Li X, Wu D and Liu L. The long intergenic noncoding RNA UFC1, a target of MicroRNA 34a, interacts with the mRNA stabilizing protein HuR to increase levels of beta-catenin in HCC cells. Gastroenterology 2015; 148: 415-426, e418.

[21] Zhou M, Zhang XY and Yu X. Overexpression of the long non-coding RNA SPRY4-IT1 promotes tumor cell proliferation and invasion by activat-

ing EZH2 in hepatocellular carcinoma. Biomed Pharmacother 2017; 85: 348-354.
[22] Li SP, Xu HX, Yu Y, He JD, Wang Z, Xu YJ, Wang CY, Zhang HM, Zhang RX, Zhang JJ, Yao Z and Shen ZY. LncRNA HULC enhances epithelial-mesenchymal transition to promote tumorigenesis and metastasis of hepatocellular carcinoma via the miR-200a-3p/ZEB1 signaling pathway. Oncotarget 2016; 7: 42431-42446.
[23] Jin W, Chen L, Cai X, Zhang Y, Zhang J, Ma D, Cai X, Fu T, Yu Z, Yu F and Chen G. Long noncoding RNA TUC338 is functionally involved in sorafenib-sensitized hepatocarcinoma cells by targeting RASAL1. Oncol Rep 2017; 37: 273-280.
[24] Yin X, Zheng SS, Zhang L, Xie XY, Wang Y, Zhang BH, Wu W, Qiu S and Ren ZG. Identification of long noncoding RNA expression profile in oxaliplatin-resistant hepatocellular carcinoma cells. Gene 2017; 596: 53-88.
[25] Colombo T, Farina L, Macino G and Paci P. PVT1: a rising star among oncogenic long noncoding RNAs. Biomed Res Int 2015; 2015: 304208.
[26] Cui M, You L, Ren X, Zhao W, Liao Q and Zhao Y. Long non-coding RNA PVT1 and cancer. Biochem Biophys Res Commun 2016; 471: 10-14.
[27] Du X, Xu MD, Wang Y, Weng WW, Wei P, Qi P, Zhang Q, Tan C, Ni S, Dong L, Yang Y, Lin W, Xu Q, Huang D, Huang Z, Ma Y, Zhang W and Sheng W. A positive feedback loop of lncRNA-PVT1 and FOXM1 facilitates gastric cancer growth and invasion. Clin Cancer Res 2017; 23: 2071-2080.
[28] Liu HT, Fang L, Cheng YX and Sun Q. LncRNA PVT1 regulates prostate cancer cell growth by inducing the methylation of miR-146a. Cancer Med 2016; 5: 3512-3519.
[29] Liu E, Liu Z and Zhou Y. Carboplatin-docetaxel-induced activity against ovarian cancer is dependent on up-regulated lncRNA PVT1. Int J Clin Exp Pathol 2015; 8: 3803-3810.
[30] Zhang XW, Bu P, Liu L, Zhang XZ and Li J. Overexpression of long non-coding RNA PVT1 in gastric cancer cells promotes the development of multidrug resistance. Biochem Biophys Res Commun 2015; 462: 227-232.
[31] Shen CJ, Cheng YM and Wang CL. LncRNA PVT1 epigenetically silences miR-195 and modulates EMT and chemoresistance in cervical cancer cells. J Drug Target 2017; 25: 637-644.
[32] Yu J, Han J, Zhang J, Li G, Liu H, Cui X, Xu Y, Li T, Liu J and Wang C. The long noncoding RNAs PVT1 and uc002mbe.2 in sera provide a new supplementary method for hepatocellular carcinoma diagnosis. Medicine (Baltimore) 2016; 95: e4436.
[33] Ding C, Yang Z, Lv Z, Du C, Xiao H, Peng C, Cheng S, Xie H, Zhou L, Wu J and Zheng S. Long non-coding RNA PVT1 is associated with tumor progression and predicts recurrence in hepatocellular carcinoma patients. Oncol Lett 2015; 9: 955-963.
[34] Wang F, Yuan JH, Wang SB, Yang F, Yuan SX, Ye C, Yang N, Zhou WP, Li WL, Li W and Sun SH. Oncofetal long noncoding RNA PVT1 promotes proliferation and stem cell-like property of hepatocellular carcinoma cells by stabilizing NOP2. Hepatology 2014; 60: 1278-1290.
[35] Xu X, Wang X, Fu B, Meng L and Lang B. Differentially expressed genes and microRNAs in bladder carcinoma cell line 5637 and T24 detected by RNA sequencing. Int J Clin Exp Pathol 2015; 8: 12678-12687.
[36] Li Q, Ge X, Xu X, Zhong Y and Qie Z. Comparison of the gene expression profiles between gallstones and gallbladder polyps. Int J Clin Exp Pathol 2014; 7: 8016-8023.
[37] Subramanian Y, Kaliyappan K and Ramakrishnan KS. Facile hydrothermal synthesis and characterization of Co2GeO4/r-GO@C ternary nanocomposite as negative electrode for Li-ion batteries. J Colloid Interface Sci 2017; 498: 76-84.
[38] Fu L, Xu Y, Hou Y, Qi X, Zhou L, Liu H, Luan Y, Jing L, Miao Y, Zhao S, Liu H and Li X. Proteomic analysis indicates that mitochondrial energy metabolism in skeletal muscle tissue is negatively correlated with feed efficiency in pigs. Sci Rep 2017; 7: 45291.
[39] Adler P, Kolde R, Kull M, Tkachenko A, Peterson H, Reimand J and Vilo J. Mining for coexpression across hundreds of datasets using novel rank aggregation and visualization methods. Genome Biol 2009; 10: R139.
[40] Dinh TA, Vitucci EC, Wauthier E, Graham RP, Pitman WA, Oikawa T, Chen M, Silva GO, Greene KG, Torbenson MS, Reid LM and Sethupathy P. Comprehensive analysis of the cancer genome atlas reveals a unique gene and non-coding RNA signature of fibrolamellar carcinoma. Sci Rep 2017; 7: 44653.
[41] Seiler R, Black PC, Thalmann G, Stenzl A and Todenhofer T. Is The Cancer Genome Atlas (TCGA) bladder cancer cohort representative of invasive bladder cancer? Urol Oncol 2017; 35: 458, e1-458, e7.
[42] Gao H, Wang H and Yang W. Identification of key genes and construction of microRNA-mRNA regulatory networks in multiple myeloma by integrated multiple GEO datasets using bioinformatics analysis. Int J Hematol 2017; 106: 99-107.
[43] Ashburner M, Ball CA, Blake JA, Botstein D, Butler H, Cherry JM, Davis AP, Dolinski K, Dwight SS, Eppig JT, Harris MA, Hill DP, Issel-

Tarver L, Kasarskis A, Lewis S, Matese JC, Richardson JE, Ringwald M, Rubin GM and Sherlock G. Gene ontology: tool for the unification of biology. The Gene Ontology Consortium. Nat Genet 2000; 25: 25-29.

[44] Ge QM, Huang CM, Zhu XY, Bian F and Pan SM. Differentially expressed miRNAs in sepsis-induced acute kidney injury target oxidative stress and mitochondrial dysfunction pathways. PLoS One 2017; 12: e0173292.

[45] Rhodes DR, Kalyana-Sundaram S, Mahavisno V, Varambally R, Yu J, Briggs BB, Barrette TR, Anstet MJ, Kincead-Beal C, Kulkarni P, Varambally S, Ghosh D and Chinnaiyan AM. Oncomine 3.0: genes, pathways, and networks in a collection of 18,000 cancer gene expression profiles. Neoplasia 2007; 9: 166-180.

[46] Tsai MC, Manor O, Wan Y, Mosammaparast N, Wang JK, Lan F, Shi Y, Segal E and Chang HY. Long noncoding RNA as modular scaffold of histone modification complexes. Science 2010; 329: 689-693.

[47] Zheng X, Hu H and Li S. High expression of lncRNA PVT1 promotes invasion by inducing epithelial-to-mesenchymal transition in esophageal cancer. Oncol Lett 2016; 12: 2357-2362.

[48] You L, Chang D, Du HZ and Zhao YP. Genome-wide screen identifies PVT1 as a regulator of Gemcitabine sensitivity in human pancreatic cancer cells. Biochem Biophys Res Commun 2011; 407: 1-6.

[49] Song LJ, Liu Q, Meng XR, Li ShL, Wang LX, Fan QX, Xuan XY. DLC-1 is an independent prognostic marker and potential therapeutic target in hepatocellular cancer. Diagn Pathol 2016; 11: 19.

[50] Ng IO, Liang ZD, Cao L and Lee TK. DLC-1 is deleted in primary hepatocellular carcinoma and exerts inhibitory effects on the proliferation of hepatoma cell lines with deleted DLC-1. Cancer Res 2000; 60: 6581-6584.

[51] Kim W, Khan SK and Yang Y. Interacting network of Hippo, Wnt/beta-catenin and Notch signaling represses liver tumor formation. BMB Rep 2017; 50: 1-2.

[52] Zhang X, Fan Q, Li Y, Yang Z, Yang L, Zong Z, Wang B, Meng X, Li Q, Liu J and Li H. Transforming growth factor-beta1 suppresses hepatocellular carcinoma proliferation via activation of Hippo signaling. Oncotarget 2017; 8: 29785-29794.

[53] Shen L, Wen J, Zhao T, Hu Z, Song C, Gu D, He M, Lee NP, Xu Z and Chen J. A genetic variant in large tumor suppressor kinase 2 of Hippo signaling pathway contributes to prognosis of hepatocellular carcinoma. Onco Targets Ther 2016; 9: 1945-1951.